Author(s): Graczykowski, B. & Mielcarek, S. & Trzaskowska, A. & Sarkar, J. & Hakonen, Pertti J. & Mroz, B.

Title: Tuning of a hypersonic surface phononic band gap using a nanoscale two-dimensional lattice of pillars

Year: 2012

Version: Final published version

Please cite the original version:

Graczykowski, B. & Mielcarek, S. & Trzaskowska, A. & Sarkar, J. & Hakonen, Pertti J. & Mroz, B. 2012. Tuning of a hypersonic surface phononic band gap using a nanoscale two-dimensional lattice of pillars. Physical Review B. Volume 86, Issue 8. 085426/1-6. ISSN 1098-0121 (printed). DOI: 10.1103/physrevb.86.085426

Tuning of a hypersonic surface phononic band gap using a nanoscale two-dimensional lattice of pillars

B. Graczykowski,[1] S. Mielcarek,[1] A. Trzaskowska,[1] J. Sarkar,[2] P. Hakonen,[2] and B. Mroz[1,3]

[1]*Faculty of Physics, Adam Mickiewicz University, Umultowska 85, 61-614 Poznan, Poland*

[2]*Low Temperature Laboratory, Aalto University School of Science, P.O. Box 15100, FI-00076 AALTO, Finland*

[3]*The NanoBioMedical Centre, Adam Mickiewicz University, Umultowska 85, 61-614 Poznan, Poland*

(Received 20 February 2012; revised manuscript received 23 May 2012; published 15 August 2012)

We present experimental and theoretical evidence of a phononic band gap in a hypersonic range for thermally activated surface acoustic waves in two-dimensional (2D) phononic crystals. Surface Brillouin light scattering experiments were performed on the (001) surface of silicon, loaded with a 2D square lattice of 100- or 150-nm-high aluminum pillars with a spacing of 500 nm. The surface Brillouin light scattering spectra revealed a different type of surface mode, related to the modulation of the lattice structure and the mechanical eigenmodes of the pillars. The experimental data were in excellent agreement with theoretical calculations performed using the finite-element method.

DOI: 10.1103/PhysRevB.86.085426 PACS number(s): 78.35.+c, 62.30.+d, 43.35.Pt, 02.70.Dh

I. INTRODUCTION

Periodically modulated composite structures made of materials of different physical properties have been under intense study lately. Such composite structures comprise photonic crystals made of components of different permittivity,[1–4] magnonic crystals that are ferromagnetics of different permeability,[5,6] and phononic crystals.[7–22] In phononic crystals of a heterogeneous one-dimensional (1D), 2D, or 3D structure, the elastic (acoustic) waves propagating in the medium are not simple plane waves that can be classified as transverse and longitudinal (or quasitransverse and quasilongitudinal). With a proper choice of material parameters and modulation spacing, it is possible to induce a complete band gap for which propagation of acoustic waves of arbitrary polarization and wave vector is forbidden. Contrary to the linear dispersion relation in the long-wavelength limit, a mechanical wave of a wavelength comparable to the spacing may undergo multiple scattering at the interfaces of different elastic media, which leads to destructive interference and to the appearance of bands of forbidden frequencies at which propagation of mechanical waves is not allowed.[7–22]

A huge part of the advanced technological solutions in electronic devices is implemented on silicon substrates. A two-dimensional periodic nanostructure in the form of pillars deposited on such a substrate, or holes (inclusions) made in the substrate, enables the control of heat flow[13] and propagation of hypersonic surface acoustic waves (SAWs).[17–20] In the surface phononics, the frequency band gap can be controlled by the filling factor, spacing, the elastic properties of the pillars/inclusions, and also the height of the pillar, which is considered in this paper. This paper presents experimental results obtained by surface Brillouin light scattering spectroscopy (SBLS)[23–25] supported by theoretical modeling by the finite-element method (FEM)[26] for a 2D aluminum hypersonic phononic structure on silicon substrate. Theoretical considerations concerning SAWs propagating in similar materials can be found in Refs. 27–30. The SAWs in phononic crystals were also studied experimentally (see, e.g., Refs. 31 and 32).

II. EXPERIMENT

The (001) surface of a pure Si substrate was coated by a 200-nm-thick poly(methyl methacrylate) (PMMA) layer and cut into chips of size 5×5 mm. Several areas of the size 100×200 μm were patterned by e-beam lithography using a JEOL 6400 instrument on each chip. The chip developed in methyl isobutyl ketone and isopropyl alcohol (MIBK:IPA)(1:3) solution was coated in an UHV evaporator with an Al metal sheet at a speed of 3 Å/s. The metal thickness of the chip was controlled by a thickness monitor, so each chip had a well defined height of a nanostructure. After evaporation, the chip was subjected to a lift-off and cleaning process. The topography of the area and the height of the pillars were measured by an atomic force microscope (AFM) (see Fig. 1). SBLS measurements were performed for the samples with a nanostructure of the period $a = 500$ nm. The shape of the pillar was approximated by that of a thimble (truncated cone) of the base radius $r = 95$ nm, semiangle $\delta = 16^\circ$, and height $b = 100$ nm (sample 1) or $b = 150$ nm (sample 2). Figure 2 presents a pillar and the unit cell assumed in FEM simulations. The calculations were performed for the elastic constants of cubic silicon $C_{11} = 165.7$ GPa, $C_{12} = 63.9$ GPa, $C_{44} = 79.9$ GPa, and density $\rho_{\mathrm{Si}} = 2331$ kg/m^3, and of isotropic aluminum $C_{11} = 111.3$ GPa, $C_{12} = 59.1$ GPa, and $\rho_{\mathrm{Al}} = 2700$ kg/m^3.[33,34]

SBLS is a nondestructive method that enables an investigation of thermally excited SAWs in the hypersonic range. SBLS provides information on the relative change in the frequency of laser light undergoing inelastic scattering by SAWs. For SAWs, the main contribution to the scattered light comes from the surface ripple mechanism rather than from the elasto-optic effect (the main contribution for bulk acoustic waves).[23,24]

SBLS measurements were performed on a six-pass tandem type Fabry-Pérot interferometer (JRS Scientific Instruments) using p-p (light polarization parallel to the plane of incidence) backscattering geometry. The source of light was a 200 mW laser generating light at $\lambda = 532$ nm. The light was collected by using f/8 optics, with a focal length of 58 mm. The solid angle of the lens was 0.63 steradians. In backscattering

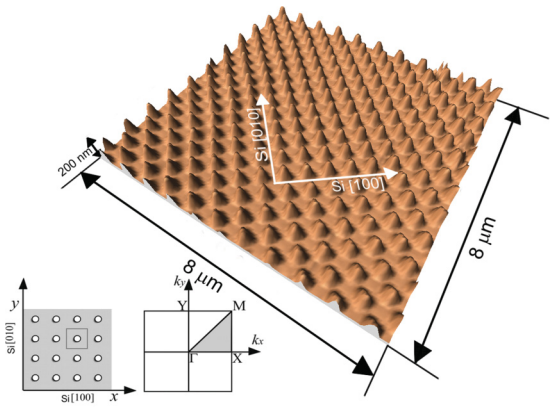

FIG. 1. (Color online) 2D pillar lattice Al on the (001) surface of Si substrate AFM topography with the crystalline orientation marked.

geometry, the angle of the laser beam incidence onto a given surface studied is equal to the scattering angle and denoted by θ. For homogeneous materials, the scattering wave vector $\mathbf{q} = \mathbf{k}_s - \mathbf{k}_i$ ($\mathbf{k}_s$ and $\mathbf{k}_i$ are wave vectors of a scattered photon and an incident photon, respectively) and the wave vector $\mathbf{k}$ of a surface phonon are equal. In such a case, the magnitude of $\mathbf{q}$ is given by[23–25]

$$q = \frac{4\pi \sin\theta}{\lambda}. \tag{1}$$

For periodic structures such as surface phononic crystals, the scattering wave vector is defined by momentum conservation:[14]

$$\mathbf{q} = \mathbf{k} + \mathbf{G}, \tag{2}$$

where $\mathbf{G}$ denotes the reciprocal lattice vector. For the considered ΓX direction, we have $q = k + 2n\pi/a$, where n is an integer. A detailed description of the experimental setup can be found in Refs. 24 and 25. SBLS measurements were performed at room temperature for θ varied in the range 14°–85° [which corresponds approximately, according to (1), to the range of wave numbers q: 0.0057–0.0235 nm^{-1}] backscattering geometry.[33,34]

III. FEM MODEL

To get a correct dispersion relation for the surface acoustic waves in the FEM approach, the boundary conditions of the unit cell (see Fig. 2) must be chosen to correspond to the physical properties of the waves. The exponential decay of the wave amplitude with depth was achieved by assuming free boundary conditions for B6 and all pillar's walls and fixed boundary conditions for the B5 wall. The height of the unit cell is dependent on the SAW length, λ_{SAW}. On the basis of preliminary simulations for silicon without a phononic nanostructure, it was assumed that $h = 2\lambda_{\mathrm{SAW}}$.[35] Such a choice of h and a fixed boundary condition for the B5 wall mean that FEM solutions are limited to surface excitations with a penetration depth smaller than $2\lambda_{\mathrm{SAW}}$. For the walls B1, B2, B3, and B4, the Bloch-Floquet[36] periodic boundary conditions were specified for each of the three components of

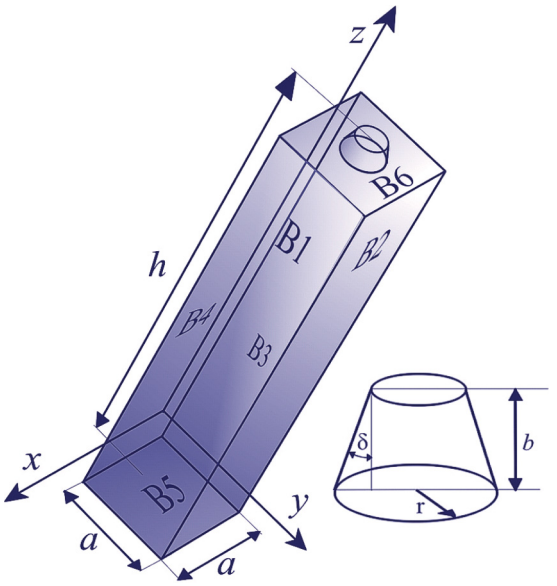

FIG. 2. (Color online) Schematic presentation of the unit cell and pillar.

deformation:

$$\begin{aligned} &u\ \exp[i(k_x x + k_y y + k_z z)],\\ &v\ \exp[i(k_x x + k_y y + k_z z)],\\ &w\ \exp[i(k_x x + k_y y + k_z z)], \end{aligned} \tag{3}$$

where u, v, and w stand for the components of deformation in the rectangular system of coordinates, and the wave vector $\mathbf{k} = (k_x,k_y,k_z) = (k\cos\alpha, k\cos\beta, k\cos\gamma)$. In the above expressions, α, β, and γ are the angles made by the wave vector and the x, y, and z axes of the coordinate system. For the Rayleigh-type SAW, it is assumed that k_z is zero (the wave vector of the surface wave is in the xy plane), while $\cos\beta = \sin\alpha$.

Based on the expressions of solid state mechanics, it is possible to determine the elastic free energy density of the deformed body on the unit volume:[37]

$$F = \tfrac{1}{2}\, C_{ijkl}\, u_{ij}\, u_{kl}, \tag{4}$$

where C_{ijkl} is the elasticity tensor and u_{ij} is the deformation tensor (small deformation):

$$u_{ij} = \frac{1}{2}\left(\frac{\partial u_i}{\partial x_j} + \frac{\partial u_j}{\partial x_i}\right), \tag{5}$$

where $(u_1,u_2,u_3) = (u,v,w)$ and $(x_1,x_2,x_3) = (x,y,z)$. From all the solutions of the FEM, where the undamped eigenmodes satisfy the above boundary conditions, the ones that are surface waves were chosen. The criterion of choice was that for SAWs, the deformation energy density along the z axis is centered at a distance lower than from the free surface:

$$\rho_z = \left(h - \frac{\int_V dV\, zF}{\int_V dV\, F}\right) < 0.2h. \tag{6}$$

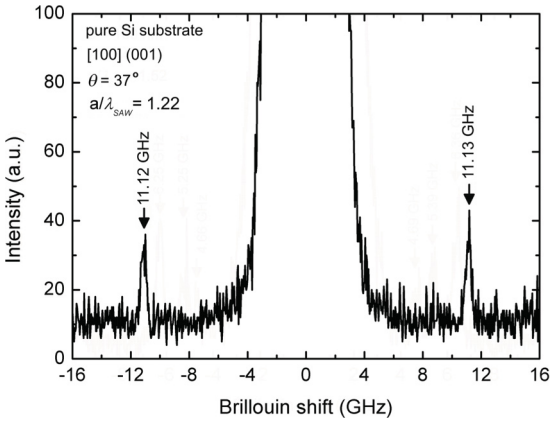

FIG. 3. SBLS spectrum for pure Si substrate. The peaks correspond to the Rayleigh surface wave propagating in the [100] direction in the (001) plane.

IV. RESULTS AND DISCUSSION

The average position of the symmetric peaks observed in the SBLS spectra provides information about the so-called Brillouin shift, which is merely the frequency of SAWs with the wave number k. In Figs. 3–5, we have particular SBLS spectra obtained for pure Si substrate, samples 1 and 2, respectively. For each sample, the spectrum provides information about SAWs propagating in the [100] direction in the (001) plane of silicon substrate.

Pure Si substrate can be considered as a typical example of a homogeneous elastic halfspace. The SBLS spectrum of the pure substrate (Fig. 3) shows only one pair of peaks related to the Rayleigh surface wave (RSW). RSW velocity generally depends on the plane and direction of propagation, the elastic constants C_{ij}, and the mass density ρ of the given material. For homogeneous, unlayered materials, RSWs (in the long-wave limit) are nondispersive.

Loading the substrate with a thin (with respect to the wavelength of the SAW) homogeneous layer can result in the appearance of other well-known types of surface excitations, e.g., Lamb, Sezawa, or Love waves, which can also be measured using SBLS. What is more, SAW velocity becomes dependent on the wave number q.[33,34]

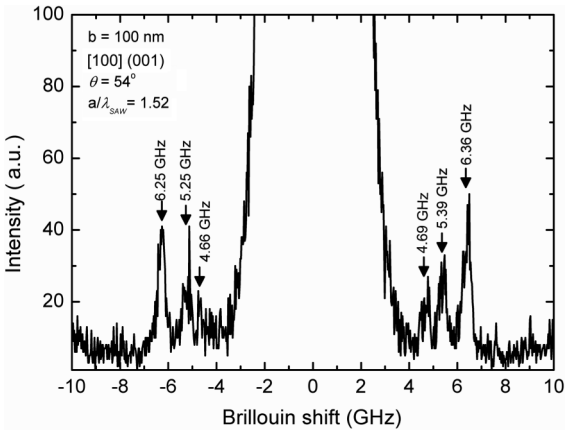

FIG. 4. SBLS spectrum obtained for sample 1 (pillars' height $b = 100$ nm).

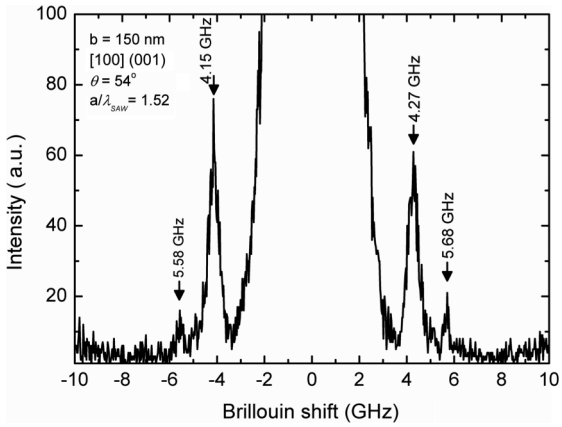

FIG. 5. SBLS spectrum obtained for sample 2 (pillars' height $b = 150$ nm).

The situation becomes more interesting if we consider the SBLS spectra obtained for samples 1 and 2 (Figs. 4 and 5) revealing the peaks that cannot be simply related to any of the surface modes mentioned. What is more, the occurrence of a pseudo-RSW propagating in the [100] direction in the (001) plane of silicon support can be neglected according to SBLS results obtained for unloaded Si substrate (Fig. 3). Generally, SBLS results obtained for several different scattering angles θ can be gathered as the dispersion relation $f_{\mathrm{SAW}}(q)$. Dispersion of SAWs can be calculated by the above-described FEM modeling taking the wave number as a parameter varied in a defined range and step. In Figs. 6–8, the SBLS data points (circles) are compared with FEM simulations (lines) for pure Si substrate, samples 1 and 2, respectively, within the range of wave numbers available in the SBLS experiment. Now, if we take into account FEM calculations for pure silicon, we have an unnatural folding effect, which comes only from periodic boundary conditions imposed on the unit cell. In addition to this unphysical effect, the SBLS results are in very good agreement with the calculations.

The dispersion relations obtained for samples 1 and 2 are much different from that typical of the unloaded surface of

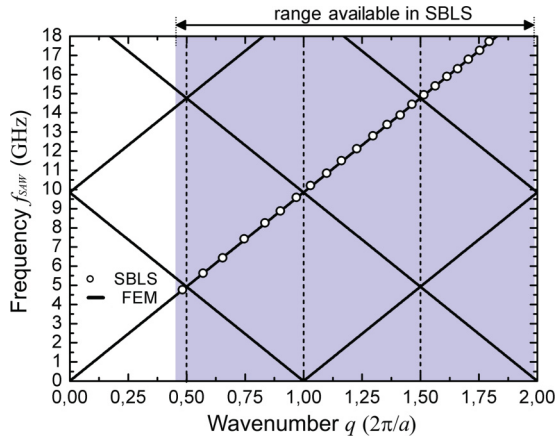

FIG. 6. (Color online) Dispersion relation for the Rayleigh surface wave propagating in the [100] direction in the (001) plane of pure Si substrate. SBLS results (circles) compared with FEM calculations (lines).

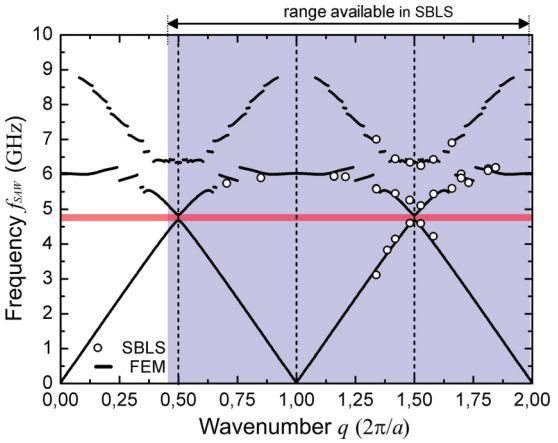

FIG. 7. (Color online) Dispersion relation for SAW obtained for sample 1. SBLS results (circles) compared with FEM calculations (lines). The hatched area denotes the band gap.

silicon (see Fig. 6). The presence of the additional peaks in the SBLS spectra mentioned above as well as the folding effect following from the experimental data cannot be explained without considering the effect of the 2D periodic lattice of pillars. According to Bloch theory,[38] wave vectors $\mathbf{k}$ and $\mathbf{k} + \mathbf{G}$ should describe the same surface mode:

$$f_{\mathrm{SAW}}(\mathbf{k}) = f_{\mathrm{SAW}}(\mathbf{k} + \mathbf{G}). \tag{7}$$

In our case, we have $f_{\mathrm{SAW}}(k) = f_{\mathrm{SAW}}(k + 2n\pi/a)$, which can be observed in dispersion relations obtained for samples 1 and 2 (Figs. 7 and 8).

Comparing SBLS spectra from Figs. 3–5, we can notice that the intensity of peaks (corresponding to SAW) for samples with aluminum pillars can be greater than that for pure silicon substrate. Generally, the intensity of light inelastically scattered on SAWs is dependent on the area of the illuminated surface spot and the reflectivity of the surface.[39] What is more, pillars can partially shadow the surface of the substrate. The effective area of the silicon, which contributes to the SBLS spectra, is reduced and depends on the pillars' dimensions and the scattering angle θ. Therefore, we can assume that the main contribution to the SBLS spectra in the samples with a 2D

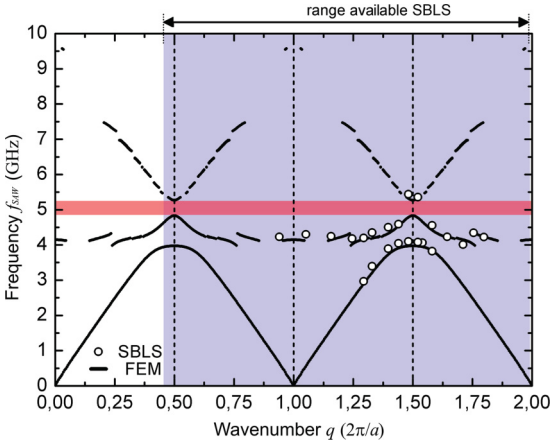

FIG. 8. (Color online) Dispersion relation for SAW obtained for sample 2. SBLS results (circles) compared with FEM calculations (lines). The hatched area denotes the band gap.

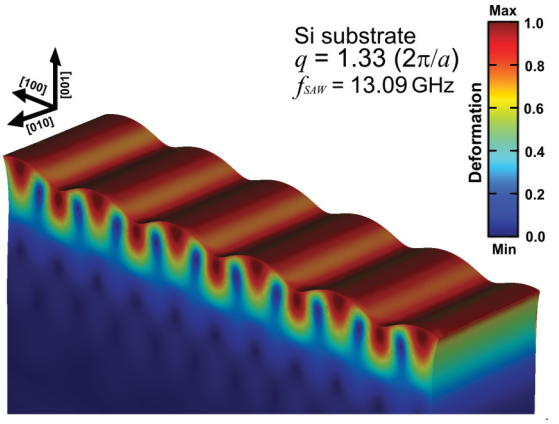

FIG. 9. (Color online) FEM three-dimensional deformation field corresponding to Rayleigh surface wave propagating in the [100] direction in the (001) plane of Si substrate.

Al nanostructure comes from metallic pillars rather than from semiconducting substrate.

The dispersion relations obtained for samples 1 and 2 reveal a series of horizontal branches corresponding to waves of very small group velocity. For these branches, the surface excitations correspond to the eigenmodes (resonant modes[28,40]) of the pillars with a simultaneous slight deformation of the silicon support (see Fig. 11). As follows from the data shown in Figs. 7 and 8, with increasing height of the pillar, the frequency of such modes decreases. Frequencies of such modes can be qualitatively explained if we make a comparison to the classical mechanics problem of a rod anchored at one end. The fundamental frequency (and other harmonics) in this case is inversely proportional to the rod height. For our samples, we have eigenmodes around 6 GHz for $b = 100$ nm and 4 GHz for $b = 150$ nm, which is in excellent agreement with the above statement. However, more general conclusions about observed modes should be confirmed by further studies for samples differing in the pillars' properties.

The FEM approach enables us to obtain a three-dimensional visualization of a given excitation. Figures 9–11 show the deformation field corresponding to the SAW (with a particular wave number) propagating in pure Si substrate, samples 1 and

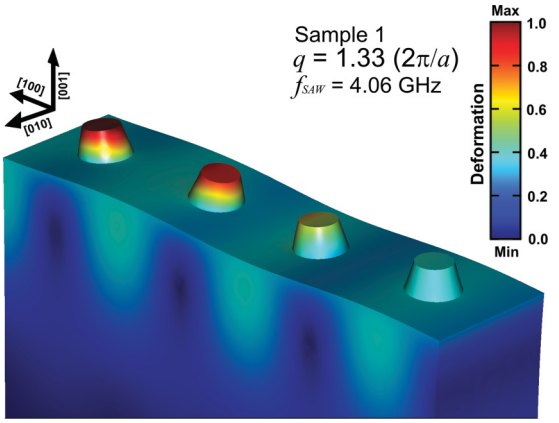

FIG. 10. (Color online) FEM three-dimensional deformation field for sample 1 corresponding to SAW propagating in the [100] direction in the (001) plane related to Si substrate.

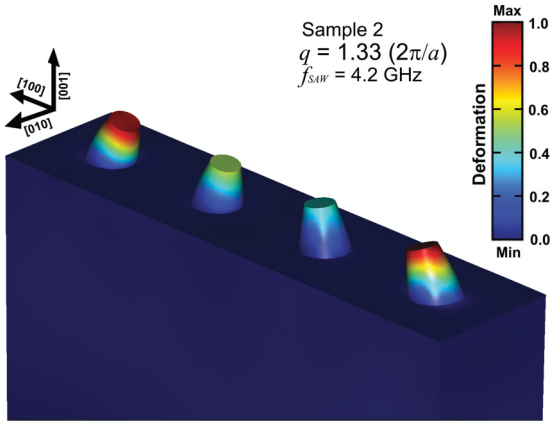

FIG. 11. (Color online) FEM three-dimensional deformation field for sample 2 corresponding to SAW propagating in the [100] direction in the (001) plane related to Si substrate.

2, respectively. Although the deformation was rescaled as we were looking for undamped eigenmodes, the scale of colors from blue to red provides insight into the character of the excitations.

A very good agreement was obtained between the SBLS experimental results and those obtained from FEM for both samples. We see that the SAW band gap for sample 1 lies in the range of frequencies 4.68–4.83 GHz, and for sample 2 we have 4.83–5.27 GHz. It can be concluded that the frequency band gap for SAWs can be tuned by the height of the pillars. For the samples studied in the present paper, we can notice that with increasing height of the pillar, the band gap width is increased and shifts toward higher frequencies. However, localized modes (here around 6 and 4 GHz in Figs. 7 and 8, respectively) can affect the frequency gap region and lead to additional band gaps, as was reported for SAWs in Ref. 28 and for longitudinal hypersonic waves in Ref. 41.

Let us consider the reflecting properties of the structure studied for SAWs. By analogy to the bulk phononic crystals, on the basis of the band structure it can be concluded that for frequencies higher than ∼9 GHz, this structure should be an excellent SAW reflector. However, it should be noted that the periodic structure of the medium can cause a transformation of the surface wave into a pseudosurface or bulk wave, and mechanical energy can be taken from the surface into the bulk. The pillars on the surface can also behave as resonators absorbing mechanical energy.[40] In such situations, we should look for such band gaps for which the surface wave energy will be scattered to a minimum degree. A tempting possibility is to simulate the propagation of surface waves in the composite structure studied in the time domain.

Surprisingly, the SBLS spectra show only selected branches of the band structure predicted by the theory. A possible explanation is that the SBLS experiment permits an observation of only such waves for which the energy of associated deformation is concentrated at the free surface. However, a detailed explanation of such behavior requires a deeper theoretical analysis, taking into account the dependence of the scattering cross section on the scattering angle.

V. CONCLUSIONS

In conclusion, we have shown that SBLS is an excellent tool that enables an investigation of SAWs in the hypersonic surface phononic crystals. We have obtained experimental evidence on the thermally excited SAW phononic band gap in the structures considered. We have employed SBLS to investigate the possibility of tuning SAW propagation by the height of the overlaid pillar structures. Deposition of a periodic 2D nanostructure in the form of aluminum pillars on the silicon substrate radically changed the dispersion relation of SAWs with respect to that observed for an unloaded silicon surface. The SBLS spectra indicate that with increasing height of the pillars, the band gap width is increased and simultaneously shifted toward higher frequencies. What is more, we have observed low-frequency surface modes with very low group velocity, which are related to the pillars' mechanical eigenmodes coupled with silicon substrate. FEM calculations, which accurately reproduce the experimental dispersion relation, yield a detailed 3D mapping of the elastic deformations. Altogether, we have established that FEM and SBLS together offer the possibility of a theoretical design and an experimental examination of surface phononic devices with desired band gap properties. These can be applied to high-tech electronic devices working with GHz frequencies.

ACKNOWLEDGMENTS

This work has been partially supported by Grant No. N202 230637 from the Polish Ministry of Science and Higher Education. The work of J.S. and P.H. was supported by the Academy of Finland.

[1]E. Yablonovitch, Phys. Rev. Lett. **58**, 2059 (1987).
[2]E. Yablonovitch and T. J. Gmitter, Phys. Rev. Lett. **63**, 1950 (1989).
[3]M. Maldovan and E. L. Thomas, Nat. Mater. **3**, 593 (2004).
[4]J. E. Wijnhoven and V. L. Vos, Science **281**, 802 (1998).
[5]V. E. Demidov, S. O. Demokritov, and B. Hillebrands, *Spin Dynamics in Magnetic Nanostructures: Micro-Brillouin Light Scattering Spectroscopy in Encyclopedia of Materials: Science and Technology* (Elsevier, Amsterdam, 2008).
[6]A. A. Serga, A. V. Chumak, and B. J. Hillebrands, J. Phys. D **43**, 264002 (2010).
[7]F. R. Montero de Espinosa, E. Jimenez, and M. Torres, Phys. Rev. Lett. **80**, 1208 (1998).
[8]M. Kafesaki and E. N. Economou, Phys. Rev. B **60**, 11993 (1999).
[9]R. Sainidou, N. Stefanou, and A. Modinos, Phys. Rev. B **66**, 212301 (2002).
[10]M. Maldovan and E. L. Thomas, *Periodic Materials and Interference Lithography* (Wiley-VCH, Weinheim, 2006).

[11] Y. Pennec, J. O. Vasseur, B. Djafari-Rouhani, L. Dobrzyński, and P. A. Deymier, Surf. Sci. Rep. **65**, 229 (2010).
[12] W. Cheng, N. Gomopoulos, G. Fytas, T. Gorishnyy, J. Walish, E. L. Thomas, A. Hiltner, and E. Baer, Nano Lett. **8**, 1423 (2008).
[13] P. E. Hopkins, C. M. Reinke, M. F. Su, R. H. Olsson III, E. A. Shaner, Z. C. Leseman, J. R. Serrano, L. M. Phinney, and I. El-Kady, Nano Lett. **11**, 107 (2011).
[14] N. Gomopoulos, D. Maschke, C. Y. Koh, E. L. Thomas, W. Tremel, H. J. Butt, and G. Fytas, Nano Lett. **10**, 980 (2010).
[15] V. Laude, M. Wilm, S. Benchabane, and A. Khelif, Phys. Rev. E **71**, 036607 (2005).
[16] J. O. Vasseur, P. A. Deymier, B. Chenni, B. Djafari-Rouhani, L. Dobrzynski, and D. Prevost, Phys. Rev. Lett. **86**, 3012 (2001).
[17] Y. Tanaka and S. I. Tamura, Phys. Rev. B **58**, 7958 (1998).
[18] Y. Tanaka and S. I. Tamura, Phys. Rev. B **60**, 13294 (1999).
[19] T. T. Wu, Z. G. Huang, and S. Lin, Phys. Rev. B **69**, 094301 (2004).
[20] D. Nardi, M. Travagliati, M. E. Siemens, Q. Li, M. M. Murnane, H. C. Kapteyn, G. Ferrini, F. Parmigiani, and F. Banfi, Nano Lett. **11**, 4126 (2011).
[21] M. S. Kushwaha, P. Halevi, L. Dobrzynski, and B. Djafari-Rouhani, Phys. Rev. Lett. **71**, 2022 (1993).
[22] M. M. Sigalas and E. N. Economou, Solid State Commun. **86**, 141 (1993).
[23] J. D. Comins, *Handbook of Elastic Properties of Solids, Liquids and Gases* (Academic, San Diego, 2001), Vol. 1.
[24] J. R. Sandercock, *Trends in Brillouin Scattering*, Topics in Applied Physics Vol. 51 (Springer, Berlin, 1982).
[25] B. Mroz and S. Mielcarek, J. Phys. D **34**, 395 (2001).
[26] R. W. Pryor, *Multiphysics Modeling Using COMSOL: A First Principles Approach* (Jones and Bartlett, Sudbury, MA, 2009).
[27] M. B. Assouar and M. Oudich, Appl. Phys. Lett. **99**, 123505 (2011).
[28] A. Khelif, Y. Achaoui, S. Benchabane, V. Laude, and B. Aoubiza, Phys. Rev. B **81**, 214303 (2010).
[29] Y. Pennec, B. Djafari-Rouhani, H. Larabi, J. O. Vasseur, and A. C. Hladky-Hennion, Phys. Rev. B **78**, 104105 (2008).
[30] T.-T. Wu, Z.-G. Huang, T.-C. Tsai, and T.-C. Wu, Appl. Phys. Lett. **93**, 111902 (2008).
[31] J.-F. Robillard, A. Devos, and I. Roch-Jeune, Phys. Rev. B **76**, 092301 (2007).
[32] C. Giannetti, B. Revaz, F. Banfi, M. Montagnese, G. Ferrini, F. Cilento, S. Maccalli, P. Vavassori, G. Oliviero, E. Bontempi, L. E. Depero, V. Metlushko, and F. Parmigiani, Phys. Rev. B **76**, 125413 (2007).
[33] G. W. Farnell, *Properties of Elastic Surface Waves*, Physical Acoustics 6 (Academic, New York, 1970).
[34] G. W. Farnell and E. L. Adler, *Elastic Wave Propagation in Thin Layers*, Physical Acoustics 9 (Academic, New York, 1972).
[35] B. Graczykowski, B. Mroz, S. Mielcarek, T. Breczewski, M. L. No, and J. S. Juan, J. Phys. D **44**, 455307 (2011).
[36] A. Khelif, B. Aoubiza, S. Mohammadi, A. Adibi, and V. Laude, Phys. Rev. E **74**, 046610 (2006).
[37] L. D. Landau and E. M. Lifshitz, *Theory of Elasticity* (Pergamon, New York, 1959).
[38] H. Ibach and H. Lutch, *Solid-State Physics: An Introduction to Principles of Materials Science* (Springer, Berlin, 2009).
[39] R. Loudon and J. R. Sandercock, J. Phys. C **13**, 2609 (1980).
[40] Y. Achaoui, A. Khelif, S. Benchabane, L. Robert, and V. Laude, Phys. Rev. B **83**, 104201 (2011).
[41] T. Still, W. Cheng, M. Retsch, R. Sainidou, J. Wang, U. Jonas, N. Stefanou, and G. Fytas, Phys. Rev. Lett. **100**, 194301 (2008).